NOVEL, ALL-DIGITAL PHASE MEASUREMENT SYSTEM FOR TIME SCALES

S. Römisch
NIST – Time and Frequency Division, Boulder, CO, USA
Spectral Research, Louisville, CO, USA
E-mail: *romisch@boulder.nist.gov*

T. E. Parker and S. R. Jefferts
NIST – Time and Frequency Division, Boulder, CO, USA

Abstract

A novel, all-digital phase measurement system to be utilized as part of the NIST time scale at NIST in Boulder, CO is presented. The system is used to compare output signals from different commercial atomic frequency standards; the phase differences between these signals will be fed to the algorithm used to generate the NIST time scale.

Preliminary results from common-clock measurements show a time deviation $\sigma_x(\tau) < 6 \cdot 10^{-13}$ s for measurement times up to 2000 s and below 1 ps for measurement times up to 10,000 s. Within these measurement times, and up to 250,000 s (approximately 3 days), the performance of the system is comparable to the measurement system presently integrated in UTC (NIST). A direct comparison of different clock measurements as performed by the system described in this paper and by the one that is part of UTC (NIST) is also presented as a mean of validation of the newly developed measurement system.

INTRODUCTION

The implementation of a time scale requires the ability to compare the time evolution of clock signals, which are then fed to a weighing algorithm that computes the scale. The high stability of the clocks generally involved in time-scaling operations requires high-resolution measurement systems, hence the impossibility of using currently available time-interval counters or frequency counters directly applied to the output of the clocks, and the need of sensitivity enhancement techniques.

The basic idea for comparing the phase of two clocks using a time-interval counter is summarized in Figure 1, where the waveforms are not drawn to scale and the labels START and STOP identify the time interval being measured.

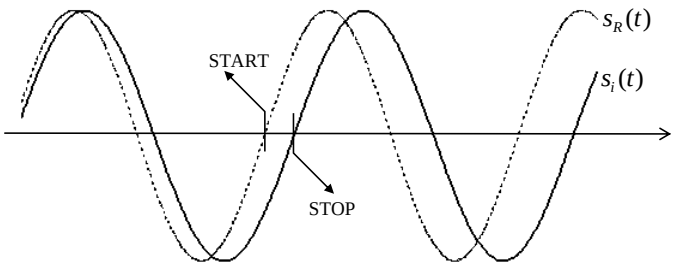

In general:

$$s(t) = V \sin \Phi(t)$$

$$\nu(t) = \frac{d\Phi(t)}{dt}$$

$$\Phi_i - \Phi_r \Big|_{t_{START}} = -2\pi \bar{\nu}_i \; t_{STOP} - t_{START}$$

Figure 1. Illustration of phase comparison by use of time-interval counters. The waveforms are not drawn to scale, and the labels START and STOP identify the time interval being measured.

A direct measurement of the time interval in the case of 5 MHz signals, as it is typically used in time scales, allows a resolution of the order of 10 ps, which leads to a phase resolution of only about $3 \cdot 10^{-4}$ radians.

The most widely used measurement technique for measuring time differences between pairs of clocks enhances the time-interval counter resolution by heterodyning the clock signals in a scheme known as the Dual-Mixer Time-Difference Measurement (DMTD) technique **[1,2]** and shown in Figure 2. The same basic idea illustrated in Figure 1 is used, but in this case $\bar{\nu}_{bi}$ is the average beat-note frequency, as shown in the bottom equation in Figure 2.

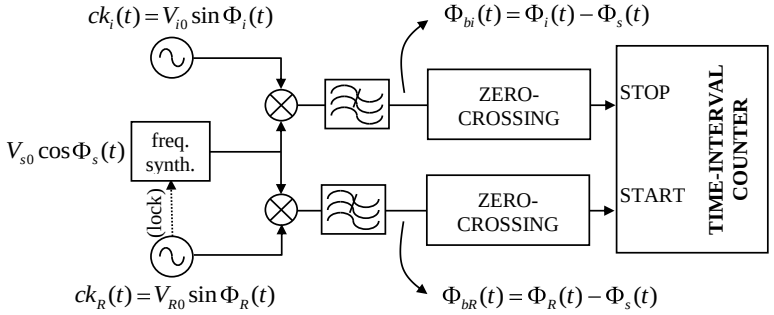

$$\nu_{s,r}(t) = \frac{d\Phi_{s,r}(t)}{2\pi\, dt}$$

$$\nu_s = \nu_R \left(1 - \frac{1}{R}\right) \text{ with } \frac{\nu_R}{R} \gg \nu_i - \nu_R$$

$$\Phi_i - \Phi_r \Big|_{t_{START}} = -2\pi \bar{\nu}_{bi} \; t_{STOP} - t_{START} \qquad \nu_{bi} \cong \nu_R / R$$

Figure 2. Block diagram illustrating the Dual-Mixer Time-Difference (DMTD) technique. The synthesized intermediate frequency ν_s is generally chosen as close as possible to the nominal frequency of all clocks, to obtain maximum sensitivity enhancement (represented by R) in the measurement of phase differences. This must be done without breaking the requirement for the resulting beat-note frequency ν_b to be large in comparison with the difference in frequency between clocks. The beat-note result of the heterodyning process is typically of the order of few Hertz, improving resolution by several hundred thousand.

The intermediate frequency ν_s is chosen to be as close as possible to the nominal frequency of all clocks, to have maximum leverage in the sensitivity enhancement mechanism. This must be done respecting the requirement for the resulting beat note to be still large when compared with the typical frequency difference between clocks. In most cases, the beat frequency resulting form the down-conversion is nominally around 10 Hz, generating a sensitivity enhancement factor R of the order of $5 \cdot 10^5$. The same time-interval measurement with a resolution of 10 ps will now yield a phase resolution around $6 \cdot 10^{-10}$ radians.

Although details in the implementation may vary, the scheme described above is still used in state-of-the-art time-difference measurement systems **[3,4]**. Advances in the capabilities of digital electronics allowed for new implementations of the traditional DMTD technique, as devised in **[5]** and in the alternative approach described in this paper.

MOTIVATION

A time scale measurement system measures time differences between pairs of clocks. These time differences are then fed to one of several possible weighing algorithms that compute the time scale itself. A time-difference measurement system is simply a phase-difference measurement system that has expanded its capability beyond the modulo-2π limitation. Nevertheless, some of the requirements for time scale measurement systems are specific and differ from the time-difference measurement systems for general applications. The first requirement regards the time elapsing between two adjacent measurements, which is required to be larger than a few seconds: for example, the UTC (NIST) time scale measures phase differences between the clocks only every 12 minutes (720 seconds). The large interval period between measurements allows each measurement to last a full second or more, significantly reducing the equivalent bandwidth of the measurement system and consequently reducing the effects of aliasing (or noise up-conversion) on the system performance.

The second requirement is that, although the system may work for different input frequencies (clocks having output frequencies of 5, 10, or 100 MHz), their nominal value is known *a priori*, greatly facilitating any kind of post-processing in the case of digitally sampled systems.

The third requirement that sets time scale measurement systems aside from the generic time-difference measurement systems is not a strictly technical one, but it is nevertheless so important as to constitute a large part of the motivation for this work. A measurement system integrated in a time scale must not lose continuity of operation over its lifetime, which is often of the order of a decade or more. To satisfy this requirement, such a system needs to be an open-source system, with full access to all its parts, enabling repairs and partial updates without loss of continuity. Moreover, these characteristics have to be functionally integrated in the system design from the beginning.

The last important requirement is not exclusive to time scale systems, but it is equally important, because it defines the maximum amount of noise allowed without invalidation of the measurement results. So far, the best clocks used to contribute to a time scale are hydrogen masers, whose relative frequency stability in terms of Allan deviation is approximately 10^{-13} at 1 s. A time-difference measurement system must therefore be stable to $\sigma_y(\tau) < 10^{-13}\ \tau^{-1/2}$ in terms of Allan deviation, or $\sigma_x(\tau) < 6 \cdot 10^{-14}\ \tau^{1/2}$ in terms of time deviation, a more apt parameter to evaluate time-difference measurement systems.

THE ALL-DIGITAL MEASUREMENT TECHNIQUE

The approach described in this paper can be summarized in one basic concept: the down-conversion performed by the analog mixers in Figure 2 is replaced by digital sub-sampling of the clock signals. The result of this operation is a digitized signal that is fitted by a sinusoidal waveform at a much lower frequency than the original clock signal.

The sub-sampling operation, like frequency mixing, preserves the phase information at the beginning of each measurement, which is the measurand of interest in the case of phase-difference measurement systems used for time scale implementation.

A graphical illustration of sub-sampling is shown in Figure 3, where all drawings are not to scale. In Figure 3 the relationship between the clock signal, the sampling clock and the resulting digitized beat-note are shown, while in Figure 4 we clarify the relationship between a *measurement window*, which yields a single *measurement point*, and τ, which is the time elapsed between two adjacent measurements.

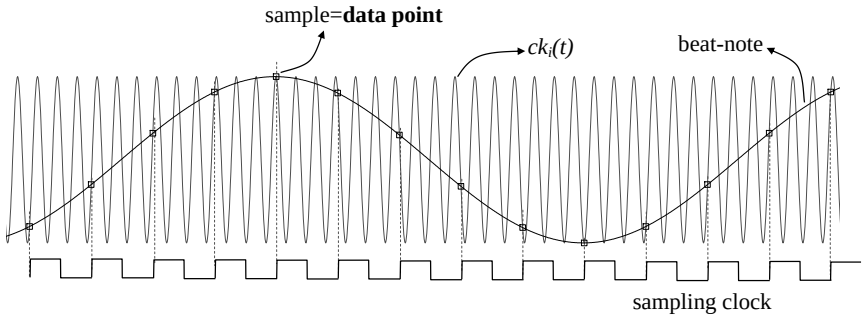

Figure 3. Graphical illustration of sub-sampling as used in the system described in this paper. The relationship between the clock signal, the sampling clock, and the resulting digitized beat-note is illustrated.

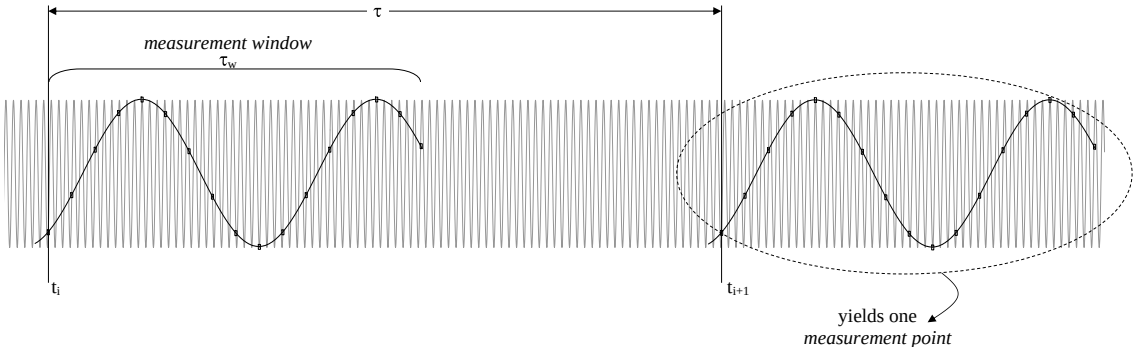

Figure 4. Graphical illustration of sub-sampling as used in the system described in this paper. We show the relationship between measurement window τ_w, yielding a single measurement point, and τ, which is the time elapsed between two adjacent measurements.

The easier way to compute the main parameters for properly sub-sampling clock signals is in the time domain, where the relationship between the clock period T_{ck} and the sampling period T_s is illustrated in Figure 5, with the help of the pictorial representation of the clock-under-measurement signal $ck_i(t)$ and the

position of two subsequent samples separated by the sampling period T_s. Here, n is the integer part of the ratio of sampling frequency to clock frequency, and ΔT is a fraction of the clock's period (T_{ck}). ΔT must also be non-zero in order for the sub-sampling process to yield a digitized sinusoid and not a DC level.

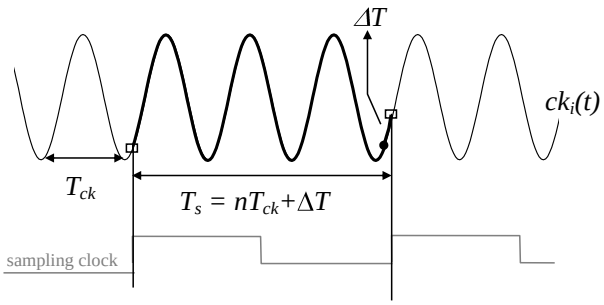

Figure 5. Relationship between the clock-under-measurement period T_s, the sampling clock period T_s, and ΔT crucial for obtaining a sinusoidal waveform from the sub-sampling process.

The choice of the sub-sampling parameters starts with the choice of the length of each measurement window τ_w and the total number of samples N acquired during it. The choice of length for the measurement window depends on the noise characteristics of both the clocks under measurement and the components of each channel, while the total number of samples N is chosen "as large as possible" considering the systems' limits in terms of acquisition and processing speed.

Without our having done yet a careful study of these factors, at this time, the values chosen for the prototype system evaluated in this paper are a measurement window τ_w of approximately 1 s with $N = 10^5$ samples.

This implies a sampling frequency of approximately 100 kHz, well within the capabilities of the system and an approximate integer ratio of the sampling frequency to the clock frequency of 50.

The choice of ΔT, the last parameter to be chosen, is made so that the N samples acquired in the measurement window τ_w will describe at least one full period of the clock signal. The constraint is written below:

$$N\,\Delta T = \eta\, T_{ck}\ ,$$

where η indicates the number of periods of the clock signal that are sampled.

From the previous two equations, two expressions may be derived, which allow the calculation of the sampling time T_s and the resulting beat-note frequency ν_{beat} from the chosen parameters n, N, and η:

$$\begin{cases} T_s = T_{ck}\,\dfrac{\eta + nN}{N} \\ \nu_{beat} = \dfrac{\eta}{\eta + nN} \end{cases}.$$

For all the measurements presented later in this paper, the parameters of the sampling system have the following values:

$$N = 10^5 \text{ samples} \quad \tau_w = 1.28 \text{ s} \quad \Rightarrow \quad 1/T_s \sim 78.125 \text{ kHz} \quad n = 64 \quad \Rightarrow \quad \eta = 4.2 \quad T_s = 12.8\ \mu\text{s} \quad \nu_{beat} = 0.328 \text{ Hz}$$

FOUR-CHANNEL PROTOTYPE SYSTEM PERFORMANCE

ARCHITECTURE

The general architecture for this all-digital, multi-channel time-difference measurement system for time scales is shown in Figure 6, where we illustrate the case of a four-channel system.

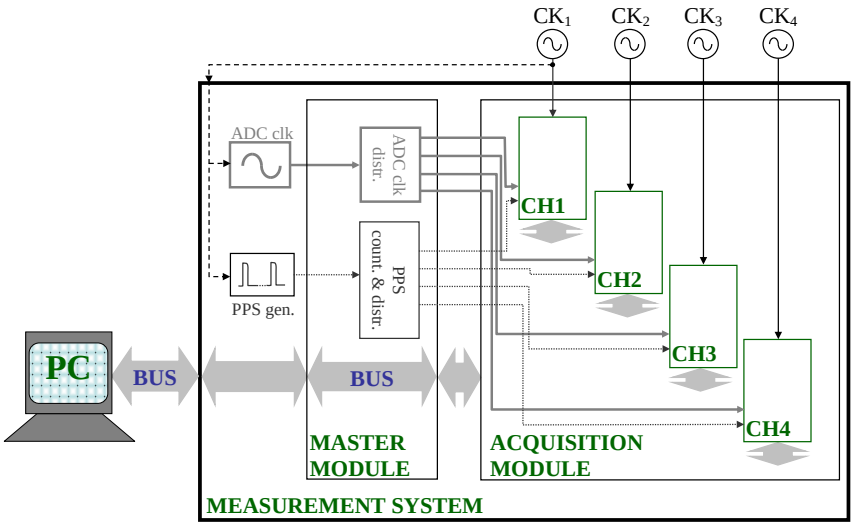

Figure 6. General architecture of an all-digital, multichannel, time-difference measurement system for time scale. The four-channel case is depicted.

Each channel module, labeled CHn, receives a copy of the Analog-to-Digital Converter's clock (ADC clk) and a copy of the Pulse-Per-Second (PPS) signal, and uses them to synchronously acquire samples from each clock CKn. Both the PPS and ADC clk signals are locked to one of the clocks-under-measurement, which doesn't have to be the reference clock for the time scale. The samples are then passed to the PC used for housekeeping and data processing by use of a common data/address bus.

The PC then implements the fitting of each set of data points (samples), providing the phase of each clock signal at the beginning of each *measurement window*. The fitting is clearly part of the measurement process, therefore contributing to the overall system performance, but we haven't yet investigated in detail how different choices would impact the final results. The results presented in this paper were obtained using a least-squares fitting to a sinusoidal function including a DC term, the fundamental component and two harmonics, using the Levenberg–Marquardt algorithm. Clearly, other methods of extracting the phase information could also be employed, including a broad range of generalized Fourier-transform-based techniques.

The Acquisition Module contains the four-channel modules, while the counting and distribution of the PPS and ADC clk signals is handled separately by the Master Module.

The specific setup for the measurements, whose preliminary results describe the performance of this system, uses three channels (CH1, CH2, and CH4) measuring the same maser (called ST0022) in a three-cornered-hat configuration, while CH3 is used to measure a different maser (called ST006).

The ADC clk and PPS signals are locked to ST0022, the maser that is measured by CH1, CH2, and CH4.

COMMON-CLOCK MEASUREMENTS

Common-clock measurements evaluate the residual noise, or noise-floor, of the measurement system. By taking the difference between the phase values coming from CH1 and CH2, the noise of the maser common to both channels is eliminated from the difference CH1-CH2, leaving the residual noise introduced by both measuring channels, which is uncorrelated. The resulting noise floor is, therefore, the combined noise of both measuring channels. In the specific case of this system, the channels' noise includes any residual error coming from the fitting process, which is considered part of the "measurement."

Two sets of measurement results are presented. The first one (1), in Figure 7(a) encompasses 13 days of continuous measurement, while the second one (2), in Figure 7(c), has a shorter duration of 3.5 days. The two sets of data represent the same pair of channels (CH1 and CH2), but they refer to different periods in time, as shown by the different Modified Julian Days (MJD) on the time axis. The quantity plotted in all the graphs in Figure 7 is the difference between the clock phase at each measurement instant, as measured by channel CH1 and CH2. It is useful to remember that each *measurement point* used to calculate phase_{CH1}-phase_{CH2} is the result of the curve-fitting of 10^5 *data points* acquired by the ADC of each channel module. The curve fitting is performed by a PC.

The longer set of data has an unaccounted (so far) event, indicated by an arrow, occurring around MJD 55140 and lasting for approximately a third of a day. For the purpose of understanding the long-term performance of the measurement system, the data points that are part of this event are eliminated from the data set before calculating the time stability yielded by the measurement. We are confident that this operation will not invalidate the performance assessment of the system over long measurement periods. Figure 7(b) shows the same data as in Figure 7(a) eliminating the portion described above.

Figure 8 shows the total time deviation calculated for both sets of data (#1 and #2) and compared with two different common-clock measurements performed by the measurement system presently integrated in UTC (NIST).

The difference between the time deviations resulting from the two data sets described in Figure 7 is not completely clear, and will be investigated in the months to come. Nonetheless, Figure 8 shows that the all-digital technique performs as well as the state-of-the-art system integrated in UTC (NIST), which also presents a certain degree of variability among the noise floors of different channels.

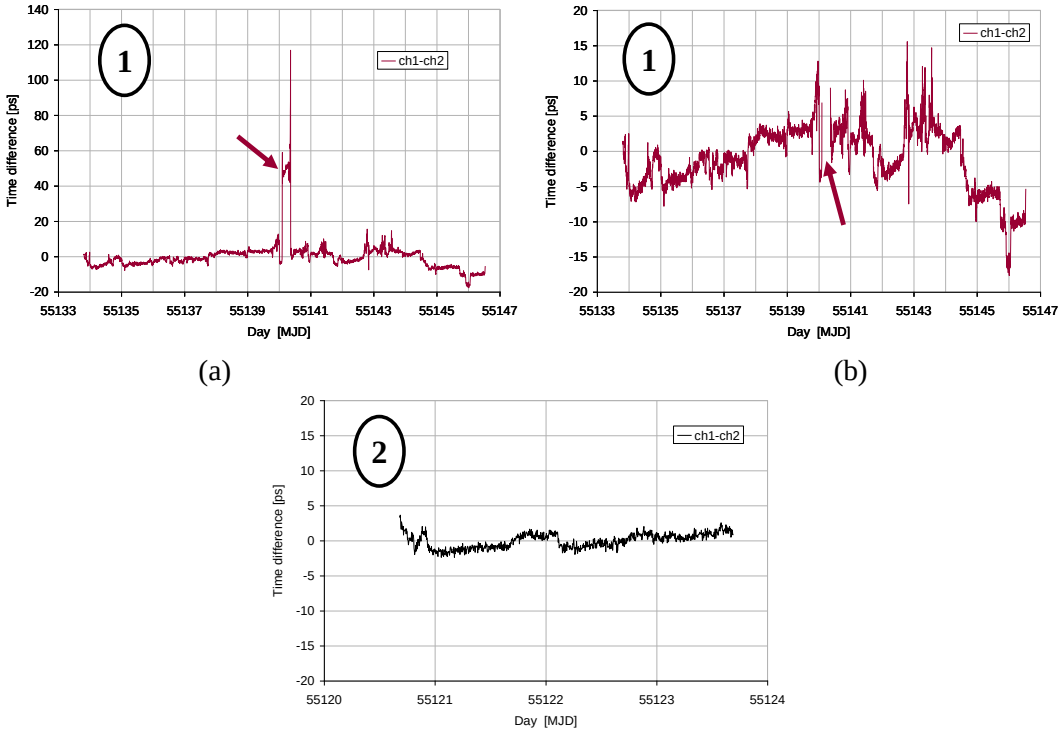

Figure 7. Results of the common-clock measurements, with maser ST0022 sampled by channels CH1, CH2, and CH4. The difference between CH1 and CH2 is shown in all the plots. (a) Complete longer (#1) data set, (b) longer data set after elimination of unaccounted event indicated by the arrow, (c) complete shorter (#2) data set.

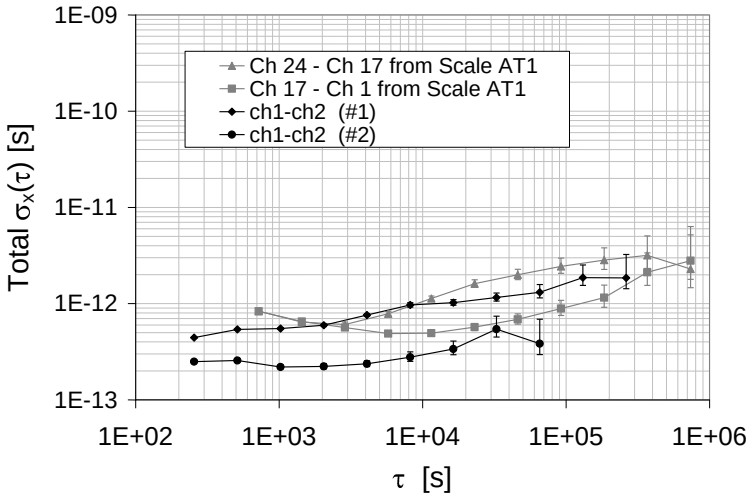

Figure 8. Total time deviation calculated for the two data sets (#1 and #2, in black) shown in Figure 7, compared with the results of common-clock measurements performed by the time-difference measurement system presently integrated in UTC(NIST) (in gray).

DIFFERENT-CLOCK MEASUREMENTS

These measurements evaluate the performance of the system in terms of normal working conditions. The two clocks are ST0022, used for the common-clock measurements and measured by CH1 for the purpose of this comparison, and ST006, measured by CH3.

The phase of each clock is measured, their difference is computed at each measurement instant, and the fractional frequency difference is calculated by use of the well-known relationships repeated below for the reader's convenience.

$$y(t) = \frac{\nu(t) - \nu_0}{\nu_0} \text{ instantaneous fractional frequency} \qquad x(t) = \frac{\varphi(t)}{2\pi\nu_0} \text{ time}$$

$$\bar{y}(t,\tau) = \frac{x(t+\tau) - x(t)}{\tau} \text{ average fractional frequency (over measurement period } \tau)$$

Finally, the average fractional frequency offset between the two clocks is calculated over the entire data set, spanning 6 days, yielding the number in the table in Figure 9. As for the common-clock measurements, we compare the results of the all-digital measurement system with the ones obtained by the system integrated in UTC (NIST), which are yielding the same average fractional frequency offset within approximately 1 part in 10^{-17}. The two measurements also yield substantially the same fractional frequency difference (the two data sets are largely coincident) shown in Figure 9(a) and the same total Allan deviation, as shown in Figure 9(b), which has the typical behavior of a maser.

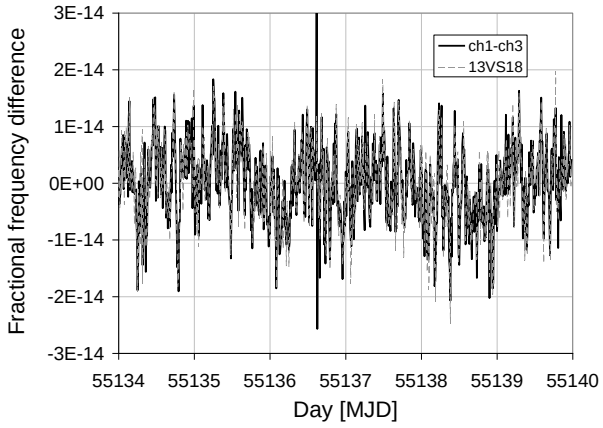

(a)

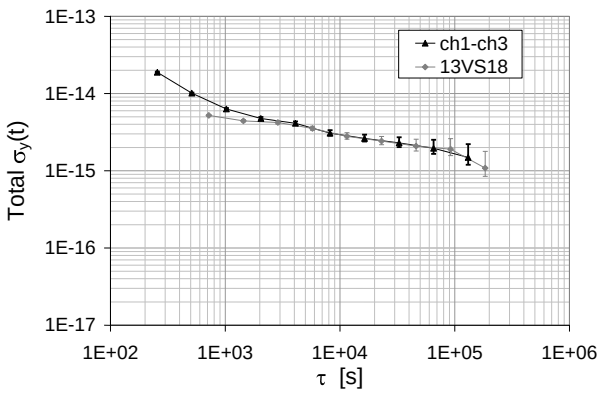

(b)

Average Fractional Frequency Offset (ST0022-ST006)	
CH1-CH3 (system described here)	-1.066563·10^{-12}
13VS18 (system integrated in UTC(NIST))	-1.066568·10^{-12}

Figure 9. Results of the frequency offset measurements as performed by the all-digital system and by the system integrated in UTC (NIST). The clocks are ST0022, measured by CH1 and ST006, measured by CH3. In (a) is shown the fractional frequency difference as a function of time as measured by both systems, while (b) shows the total Allan deviation calculated from the two data sets. In the table are reported the two values for the calculated average fractional frequency offset originated from the two data sets; they are in agreement within 5 parts in 10^{-18}.

By use of the system integrated in UTC (NIST), the fractional frequency difference between clock ST0022 and clock ST006 was found to be $-1.066568 \cdot 10^{-12}$ over the 6-day measurement period shown in Figure 8. Over that same period, the all-digital system described here measured the same two clocks to have a fractional frequency difference of $-1.066563 \cdot 10^{-12}$. The difference between these two measurements is $5 \cdot 10^{-18}$.

As a final confirmation of the level of agreement between the two systems, we calculated the total Allan deviation of the difference between the two measurements, using the data shown in Figure 9(a). The results of this calculation are shown in Figure 10 and represent the residual noise of both measurement systems, combined.

The difference of $5 \cdot 10^{-18}$ calculated from the numbers in the table of Figure 9 is shown in Figure 10 by a black four-pointed star and is consistent with the value of the total Allan deviation extrapolated to a 6-day measurement period represented by the gray dashed line in Figure 10.

CONCLUSIONS

We have presented the working principle and the performance of a novel, all-digital phase measurement system for time. The description of a four-channel working prototype is provided, along with the preliminary results of common-clock measurements and different-clock measurements. A comparison with the results of the same measurements as performed by the system presently integrated in UTC (NIST) is also provided.

The newly developed system performs comparably with the one that is part of UTC (NIST), thereby validating the all-digital technique as viable for time-difference measurement systems for time scales.

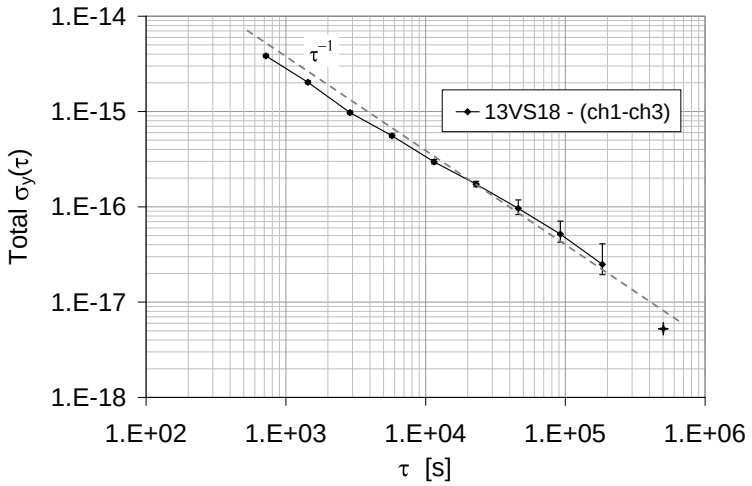

Figure 10. Total Allan deviation calculated for the difference between the two data sets shown in Figure 9. It represents the combined residual noise of the two measurement systems: the all-digital one and the one that is part of UTC (NIST). The dashed line represents a slope of τ^{-1}, used to extrapolate the measurement results up to 6 days, where it can be compared with the difference between the two average frequency offsets shown in Figure 9, represented by the black four-pointed star.

ACKNOWLEDGMENTS

The authors would like to thank T. Heavner, J. Levine, M. Lombardi, and D. Smith for helpful suggestions during the writing of this paper.

REFERENCES

[1] D. Allan and H. Daams, 1975, *"Picosecond Time Difference Measurement System,"* in Proceedings of the 1975 International Frequency Control Symposium (FCS), 28-30 May 1975, Atlantic City, New Jersey, USA (EIA, Washington, D.C.), pp. 404-411.

[2] S. Stein, D. Glaze, J. Levine, J. Gray, D. Hilliard, D. Howe, and L.A. Erb, 1983, *"Automated High-Accuracy Phase Measurement System,"* **IEEE Transactions on Instrumentation and Measurement, IM-32**, 227-231.

[3] F. Nagakawa, M. Imae, Y. Hanado, and M. Aida, 2005, *"Development of Multichannel Dual-mixer Time Difference System to Generate UTC (NICT),"* **IEEE Transaction on Instrumentation and Measurements, IM-54,** 829-832.

[4] L. Šojdr, J. Cermák, and G. Brida, 2003, *"Comparison of High-precision Frequency-stability Measurement Systems,"* in Proceedings of the 2003 International Frequency Control Symposium (FCS) & PDA Exhibition Jointly with the 17th European Frequency and Time Forum (EFTF), 5-8 May 2003, Tampa, Florida, USA (IEEE 03CH37409C), pp. 317-325.

[5] K. Mochizuki, M. Uchino, and T. Morikawa, 2007, *"Frequency-stability Measurement System Using High-speed ADCs and Digital Signal Processing,"* **IEEE Transaction on Instrumentation and Measurements, IM-56,** 1887-1893.